Robust Construction of Underwater Superoleophobic CNTs/Nanoparticles Multifunctional Hybrid Membranes via Interception Effect for Oily Wastewater Purification

Luke Yan, Gui Zhang, Lei Zhang, Wei Zhang, Jincui Gu, Youju Huang, Jiawei Zhang, Tao Chen

www.elsevier.com/locate/memsci

PII: S0376-7388(18)31803-9
DOI: https://doi.org/10.1016/j.memsci.2018.09.060
Reference: MEMSCI16505

To appear in: *Journal of Membrane Science*

Received date: 1 July 2018
Revised date: 5 September 2018
Accepted date: 26 September 2018

Cite this article as: Luke Yan, Gui Zhang, Lei Zhang, Wei Zhang, Jincui Gu, Youju Huang, Jiawei Zhang and Tao Chen, Robust Construction of Underwater Superoleophobic CNTs/Nanoparticles Multifunctional Hybrid Membranes via Interception Effect for Oily Wastewater Purification, *Journal of Membrane Science,* https://doi.org/10.1016/j.memsci.2018.09.060

Robust Construction of Underwater Superoleophobic CNTs/Nanoparticles Multifunctional Hybrid Membranes via Interception Effect for Oily Wastewater Purification

Luke Yan[a,1,*], Gui Zhang[a,1], Lei Zhang[b,*], Wei Zhang[b], Jincui Gu[b], Youju Huang[b], Jiawei Zhang[b], Tao Chen[b,*]

[a] Polymer Materials & Engineering Department, School of Materials Science & Engineering, Chang'an University, Xi'an 710064, China.

[b] Key laboratory of bio-based polymeric materials technology and application of Zhejiang province, Ningbo Institute of Materials Technology and Engineering, Chinese Academy of Sciences, Ningbo 315201, P. R. China.

E-mail: yanlk_79@hotmail.com.

E-mail: zhanglei@nimte.ac.cn

tao.chen@nimte.ac.cn.

[1] These authors contributed equally to this work.

Abstract

A simple and robust strategy is suggested for fabricating multifunctional hybrid separation membrane loading with catalytic nanoparticles based on the interception effect of porous CNTs network membrane. CNTs functionalized covalently with hydrophilic polyacrylic acid brushes assemble into a superhydrophilic/underwater superoleophobic network structure, which displays thickness dependent porosity. This allows the CNTs membrane capture catalytic nanoparticles by simple filtration process and construct flexibly desired separation membrane. Not only effectively separate oil-in-water emulsion, the prepared CNTs hybrid membranes can also catalytically decompose different organic pollutants in water by conveniently altering catalytic nanoparticles in the membrane. This robust construction provides a convenient means to obtain multifunctional CNTs separation membrane, promoting the practical application of superwettable CNTs membrane in the treatment of complex oily wastewater.

Graphic Abstract

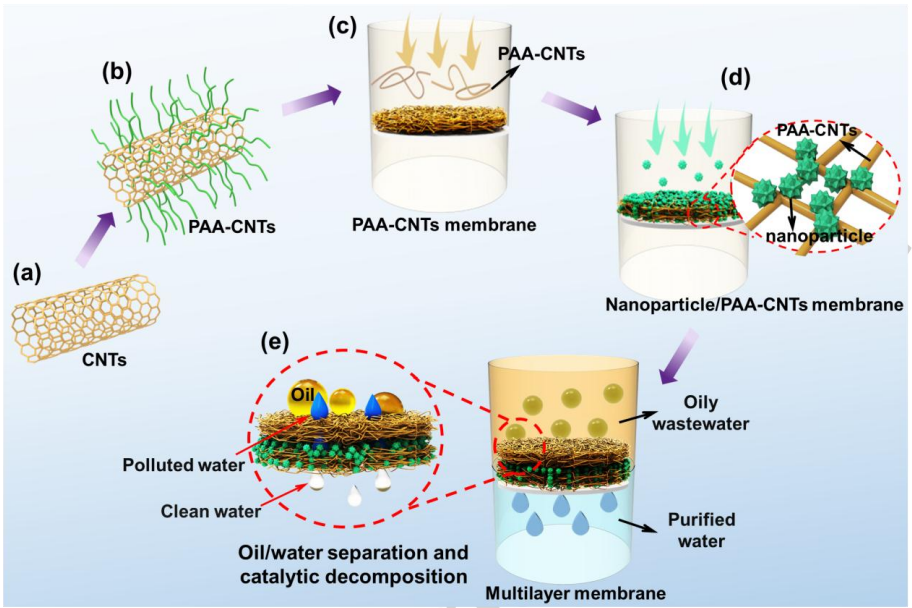

Keywords: CNTs membrane; underwater superoleophobic; oil/water emulsion separation; catalytic degradation; catalytic nanoparticles.

1. Introduction

With the rapid development of industrial and agricultural, the demand for lots of fossil fuels and various chemicals are increasing, which has caused serious environmental pollution problems all over the word for instance tainted oily wastewater [1, 2]. These oily wastewater often contain toxic organic pollutes and threaten seriously the living environment and physical health. Recently, some strategies including superwettable membrane have been developed for wastewater treatments [3-6]. Inspired by self-cleaning plants, superwettable membrane are capable of separating effectively oil or water from oil/water mixtures, and even surfactant stabilized emulsion [7-13]. For example, Jin et al reported a superhydrophilic/underwater superoleophobic polyacrylonitrile membrane with ultralow oil-adhesion for high-efficient oil/water separation [14]. Xue et al. fabricated a novel superhydrophilic and underwater superoleophobic polyacrylamide coated mesh in an oil/water/solid three-phase system, which can selectively separate water from oil/water mixtures [15]. Except these polymer membranes, superwettable inorganic carbon nanotube composite membrane or copper mesh can also achieve effectively separating oil/water mixtures and even emulsion [16]. Although most of those membrane can separate oil/water mixtures, they are inadequate to remove the organic pollutes in water. A separation membrane can purify simultaneously organic polluted wastewater during oil/water separation is highly expected [17]. To achieve removing organic pollutes, some catalytic nanomaterials are loaded in the superwettable membrane for decomposing organics [18, 19]. For example, a bilayer TiO_2-based membrane with underwater superoleophobic surface can decompose photo-catalytically organic pollutants in water, as well as separating oil from water [20]. In our previous work, superwettable CNTs network membranes or nonwoven fabric membrane loaded with catalytic nanoparticles are prepared for catalytically decomposing organics in heterogeneous emulsion during oil/water emulsion separation [21, 22].

However, the sophisticated fabrication method of these membranes remarkably limited their practical efficiency. Moreover, For example, one of the disadvantages is inconvenient alteration of the loading catalysts in the membrane dependent on various target pollutes due to the complex preparation process [23].

Superwettable carbon nanotube membrane with porous network structures have been reported to separate effectively oil/water emulsion [24-27]. More importantly, the porosity of close-packed CNTs membrane can be controlled flexibly by tuning the thickness. A CNTs network membrane with nanoscale porous structures can be used as ultrafiltration membrane to intercept nano-sized particles. This allows to load conveniently different catalytic nanoparticles into CNTs membrane by simple filtration manner, achieving multi-functional CNTs separation membrane for wastewater purification.

Herein, this work present a robust multi-functional underwater superoleophobic CNTs separation membrane loaded with model catalytic nanoparticle based on the interception effect. The resultant multilayer composite film can not only separate oil/water emulsion, and also simultaneously decompose several kinds of model organic pollutants via selecting desired catalytic nanoparticles. The fabrication strategy is schematically illustrated in Scheme 1. Hydrophilic polyacrylic acid (PAA) coated CNTs hybrid assembled into a superhydrophilic/underwater superoleophobic network membrane by vacuum filtration (Scheme 1b and 1c). Owe to the interception function of CNTs membrane, model nanoparticles such as Pd@Pt and Au nanoparticles are stably loaded in the CNTs membrane, forming a layer of catalytic membrane (Scheme 1d). Upon being covered with PAA modified CNTs membranes to avoid surface contaminate and flow impact, a sandwiched multilayer composite membrane is constructed and possesses of underwater superoleophobic surface and catalytic interlayer (Scheme 1e). The resultant composite membrane can simultaneously decomposing catalytically organic pollutants during oil/water emulsion separation (Scheme 1). This robust construction with high operability favor the catalytic function modulation of CNTs separation membrane based

on its interception effects, which is considered to promote the practical utilization of superwettable CNTs in water purification.

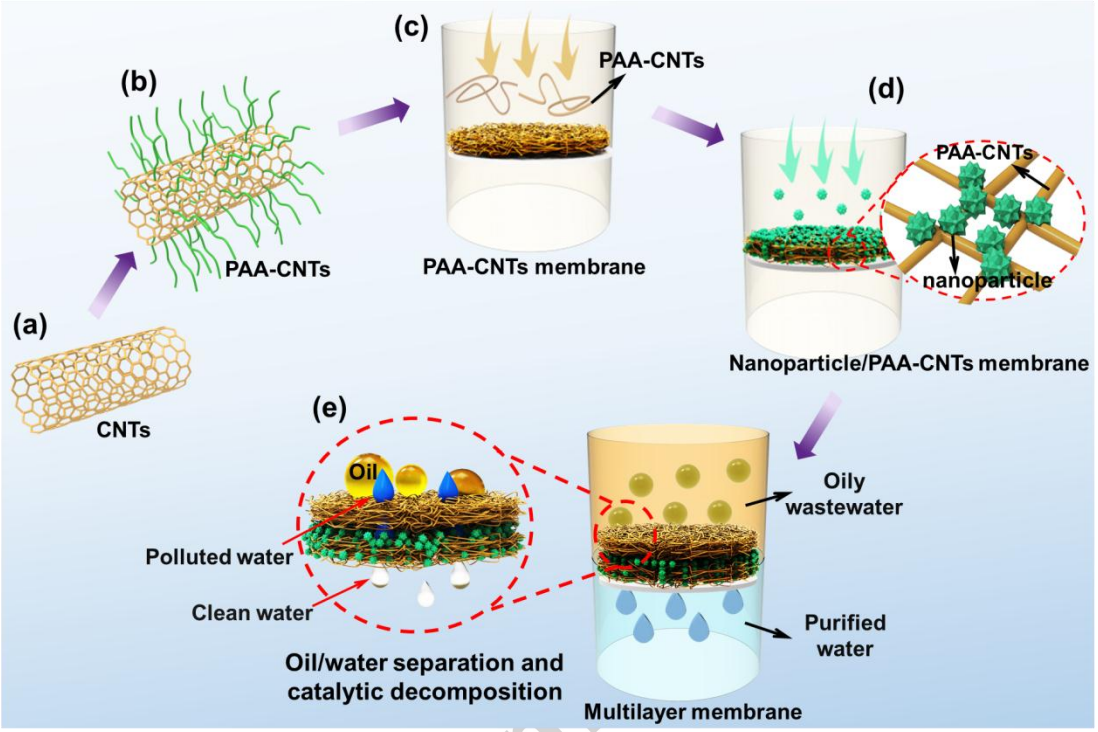

Scheme 1. Fabrication of multi-functional CNTs composite separation membrane by filtration. (a, b) PAA modified CNTs (PAA-CNTs). (c) PAA-CNTs membrane prepared by vacuum filtration. (d) The deposition of catalytic nanoparticles in PAA-CNTs membrane. (e) The resultant multilayer PAA-CNTs/Pd@Pt/PAA-CNTs composite membrane is employed for oil/water separation and catalytic decomposition.

2. Experimental section

2.1. Materials

Multi-walled carbon nanotubes (CNTs, purity >90%, 10-30 μm length and 10-30 nm diameter, 1.5 w_t% COOH group) were purchased from Chengdu Organic Chemistry Co., Ltd. Acrylic acid (AA, 99%) and benzoyl peroxide (BPO) were purchased from Alfa Aesar China (Tianjin) Co., Ltd. Pluronic F-127, potassium chloroplatinite (K_2PtCl_4), disodium tetrachloropalladate (Na_2PdCl_4), 4-nitrophenol (4-NP, 98 wt%) and methylene

blue (MB) were provided by Sigma-Aldrich (Shanghai) Co., Ltd. PVDF membranes were obtained from Millipore Industrial & Lab Chemicals (aperture about 0.45 μm, thickness about 125 μm). Soya-bean oil was obtained from the local supermarket. Other chemicals were purchased from Sinopharm Chemical Reagent Co., Ltd and used as received.

2.2. Surface functionalization of CNT by PAA brushes

Typically, 0.15 g of CNTs is dispersed into 150 mL of acetone in a 250 mL three-neck flask. After 20 min ultrasonic processing, 3.0 g of acrylic acid (AA) is added and bubbled with nitrogen for 30 min. The polymerization reaction is initiated by adding 0.065 g of benzoyl peroxide and kept at 75 ℃ for 8 h. The resultant PAA modified CNTs hybrid (PAA-CNTs) are collected by filtration and washed by deionized water to remove residual reactants. Finally, the CNTs hybrid is dried at 30 ℃ for 24 h for further using.

2.3. The Synthesis of model catalytic nanoparticles

Gold nanoparticles: According to our previous reports [21, 28, 29], the sodium citrate solution (10 mL, 33 mM) is added into 140 mL ultrapure water with continuous stirring and boiling. After that, $HAuCl_4$ (1 mL, 25 mM) and tris-base (5 mL, 0.1 M) are sequentially added (time defer 1 min) and kept in an oil bath of 137 ℃. The color of the reaction solution changes gradually from colorless to light pink, rose-red, fuchsine in a few minutes. Upon keep heating for 20 min, the temperature of the oil bath is reduced to 100 ℃. Then, 1 mL of $HAuCl_4$ (25 mM) is added and stirred continuously for another 30 min until achieving uniform nanoparticles.

Pd@Pt nanoparticles: Pluronic F-127 (10 mg) is dissolved into aqueous solution containing 20 mM of Na_2PdCl_4 (0.1 mL), 20 mM of K_2PtCl_4 (0.9 mL) solution and 6 M of hydrochloric acid (22 μL). After that, 1.0 mL of 100 mM ascorbic acid (AA) is added and the mixture is subsequently sonicated in a water bath for 30 minutes. In the process of ultrasonication, the temperature remains unchanged at 35 ℃. Finally, the product is stirred at 30 ℃ for 24 h (rotate speed: 180 rpm). The final product is collected by centrifugation and re-dispersed into deionized water.

2.4. Preparation of multilayer CNTs composite membrane

The preparation of CNTs membrane containing Pd@Pt nanoparticles is taken as an example. First, 10 mg PAA-CNTs is dispersed into 100 mL of water and 10 mL of the resultant dispersion is poured into the filtration setup equipped with PVDF membrane. A uniform PAA-CNTs membrane is obtained after filtration under 0.09 MPa of vacuum pressure. Subsequently, 0.5 mL of Pd@Pt nanoparticles solution is diluted into 20 mL deionized water and is added onto the PAA-CNTs membrane before filtrating. A resultant Pd@Pt nanoparticles layer is formed and serves as the catalyst layer of hybrid membrane (PAA-CNTs/Pd@Pt). Finally, another PAA-CNTs membrane deposits on the above hybrid membrane under same condition, achieving the PAA-CNTs/Pd@Pt/PAA-CNTs hybrid membranes.

2.5. Preparation of the oil-in-water emulsions

Oil-in-water emulsion: For oil-in-water emulsions, tween 80 (HLB = 15, an emulsifier of the oil-in-water type. 1.2, 1.1 and 1.0 g of tween 80 for toluene-in-water, chloroform-in-water, and hexane-in-water) is dissolved into 120 mL of water and stirred for 2 h. Then 4 mL of oil is added into above solution and stirred for another 3 h. The prepared emulsion stands undisturbedly for 24 h and obtain stable oil-in-water emulsion.

Toluene-in-water emulsion containing MB is taken as a model of organic polluted oily wastewater. The content of MB in emulsion is tuned according to the actual requirements and the molar ratio of $NaBH_4$/MB is kept constant of 100/1. Typically, 15 mg of MB and 0.152 g of $NaBH_4$ are added into 300 mL of prepared emulsion and stirred for 2 h to obtain stable mixed emulsion.

2.6. Oil/water emulsion separation and catalytic decomposition of pollutants

The catalytic decomposition performance of the each composite membrane is assessed using model catalytic degradation reactions. The catalytic decomposition of blue MB in the presence of $NaBH_4$ is used to verify the catalytic effect of composite

membrane containing Pd@Pt. Besides, the catalytic transformation reaction from yellow nitrophenol to colorless aminophenol is used to study the catalytic effects of composite membrane containing Au NPs. The catalytic decomposition of MB on the Pd@Pt/PAA-CNTs membrane is taken as an example. Nominally, 30 mL of emulsion containing MB or 4-NP is filtrated through the Pd@Pt/PAA-CNTs membrane under vacuum. The filtrated solution and feed emulsion are collected for further characterization.

2.7. Characterization

The microstructures of CNTs and composite membrane are characterized by scanning electron microscopy (Hitachi S4800 scanning microscope) at an acceleration voltage of 4 kV and transmission electron microscopy (FEI Tecnai F20 electronic microscope) operating at 2.0 kV. X-ray photoelectron spectroscopy (XPS) analysis is performed on a Shimadzu Axis Ultradld spectroscope, using C-O (alpha) as radiation resource. Dynamic light scattering (DLS) measurement is performed on a Zetasizer Nano ZS. Fourier transform infrared (FTIR) spectra are recorded on a Thermo-fisher Nicolet6700 spectrometer using KBr disk technique. The underwater oil contact angles (OCA) measurements are tested at environment temperature using an OCA-20 DataPhysics instrument. Pore size distribution (PSD) of hybrid membranes is evaluated by liquid-liquid porometer (LLP-1200A, Porous Materials Inc. US). The averaged value of three testing results is used to determine the pore size of membrane. UV/vis absorption spectra are recorded by virtue of TU-1810 UV/vis spectrophotometer provided by Purkinje General Instrument Co. Ltd. The average TOC content in the feed emulsion and filtrate solution were measured using a total organic carbon analyzer (Multi N/C 2100, Analytikjena, Germany).

3. Results and discussion

3.1. Characterization of PAA grafted CNTs hybrid

In order to achieve superhydrophilic/underwater superoleophobic CNTs film for separating oil/water emulsion, CNT is grafted covalently with hydrophilic PAA brushes by in-situ free radical polymerization [30]. The microstructures and composition of resultant CNTs hybrid (PAA-CNT) were characterized to verify the modification of PAA on CNTs. Fig. 1(a) and (b) show the SEM images of pristine CNTs and PAA-CNT hybrid, respectively. It is indicated that the average diameter of the PAA-CNT hybrid increase from original 25 nm to about 49 nm. The TEM image also clearly shows a layer of polymer coated on the surface of CNTs. The composition of CNTs hybrid was characterized by FT-IR spectrum (Fig. 1d). In the FT-IR spectrum of PAA-CNTs, The peak at 3441 cm^{-1} is attributed to the stretching of O-H group [31] and the peak at 2357 cm^{-1} arises from the vibration of carbon dioxide in the air [32]. The peaks at 1704 cm^{-1} and 1560 cm^{-1} nearby corresponds to the stretching vibration of carboxyl groups [33], while the peaks at 1403 cm^{-1} and 1168 cm^{-1} are assigned to C-C prop and C-O stretching in PAA respectively. These results confirm the presence of PAA brushes on CNTs.

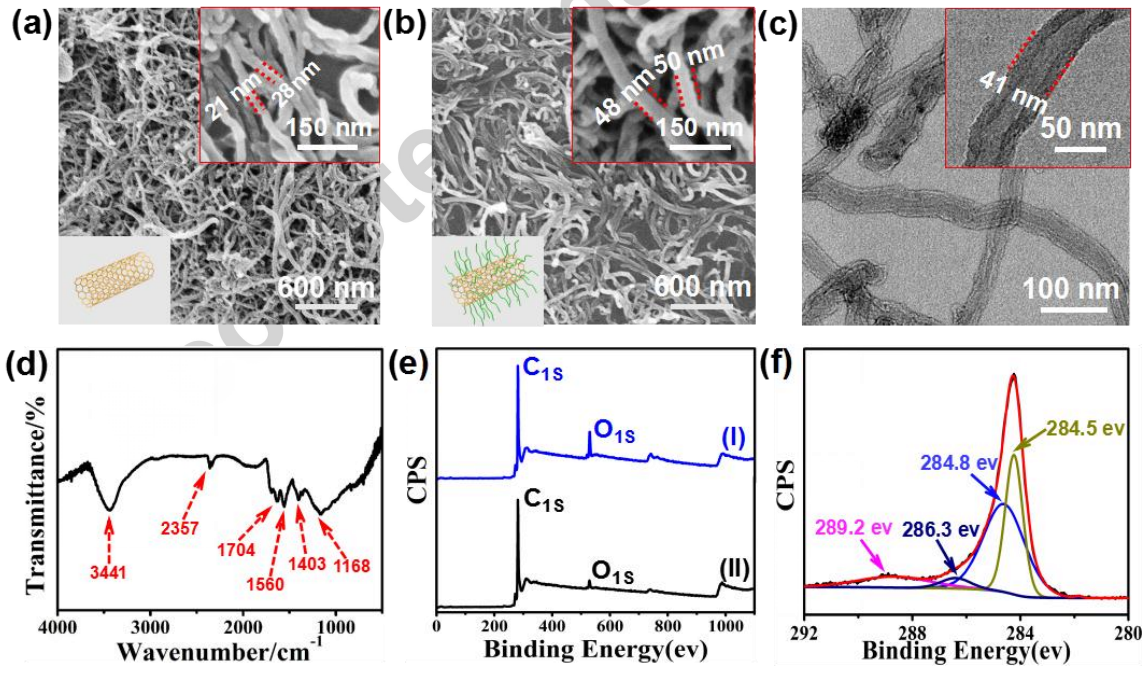

Fig. 1. SEM images of (a) pristine CNTs and (b) PAA-CNTs (The inset schemes highlight the structures of hybrid). TEM image (c) and FTIR spectrum (d) of PAA-CNTs hybrid. (e)

XPS spectra of (I) PAA-CNTs and (II) pristine CNTs. (f) C 1s spectrum of the PAA-CNTs.

In addition, the PAA-CNT hybrid was further analyzed by X-ray photoelectron spectroscopy (XPS). As shown in Fig. 1e and Fig. S1, the XPS spectrum of the PAA-CNTs hybrid exhibits (Fig. 1e) stronger O 1s signal than that of pristine CNTs. The C 1s peak can be divided into four bands (Fig. 1f) [34-37]: sp^2-hybridized carbon of CNTs at 284.5 eV, sp^3-hybridized carbon from PAA brushes at 284.8 eV, carbon singly bound to oxygen (C-O) on the oxidized CNTs at 286.3 eV, carbon bound to two oxygens in carboxyls (O-C=O) at 289.2 eV. These results confirm the successful modification of PAA on the surface of CNTs.

3.2. Surface wettability of PAA-CNTs membrane and its interception effect

Upon vacuum filtration, PAA-CNTs assemble into a uniform membrane supported on the PVDF membrane (Fig. 2a). The contact angles is used to investigate the wettability of PAA-CNTs membrane. The underwater CA of dichloromethane (CH_2Cl_2) solvent on the membrane is about 152^o (the inset in Fig. 2a), showing underwater superoleophobic feature. In addition, the PAA-CNTs membrane shows similar underwater superoleophobic wettability for other organic solvents such as chloroform ($CHCl_3$) and toluene (Fig. 2b). The microstructure of the PAA-CNTs membrane was further observed by SEM. It is showed that PAA-CNTs assemble into a porous network membrane with a uniform thickness of about 1 μm (Fig. 2c and 2d).

The permeation of CNTs membrane is closely related with its thickness, indicating the dependence of porosity of CNTs membrane on its thickness. In order to explore the relationship between the thickness and its porosity, CNTs membranes with different thickness were prepared by controlling the content of used CNTs (Fig. S2). With the increasing of thickness from 0.7 μm to 4 μm, the membrane porosity reduces gradually from 164.7 nm to 51.6 nm (Fig. 2e). This small-sized porosity exactly allows the composite membrane capture the nanoscale nanoparticles. For example, Au nanoparticles

(Au NPs) with averaged sizes of 40 nm are taken as model nanoparticles to investigate the interception of CNTs membrane. After passing through a PAA-CNTs membrane, some Au NPs are blocked on the membrane, leading to the concentration reduction of filtrated Au NPs solution. The content variation of Au NPs can be used to evaluate the interception yields of PAA-CNTs membrane. It is found that the concentration of filtrated Au solution decreases clearly with increasing the membrane thickness, showing enhanced interception efficiency. When the PAA-CNTs membrane thickness increase from 0.7 μm to 4 μm, the interception efficiency approaches as high as 87.3% for 40 nm of Au NPs (Fig. 2f). It is indicated that the CNTs composite membrane with larger thickness shows better interception performances for nanoparticles. On the other hand, the CNTs composite membranes with larger thickness usually exhibit lower flux. To balance the contradictory influences of interception and flus, PAA-CNTs membrane with 1 μm of thickness is selected as an optimal model.

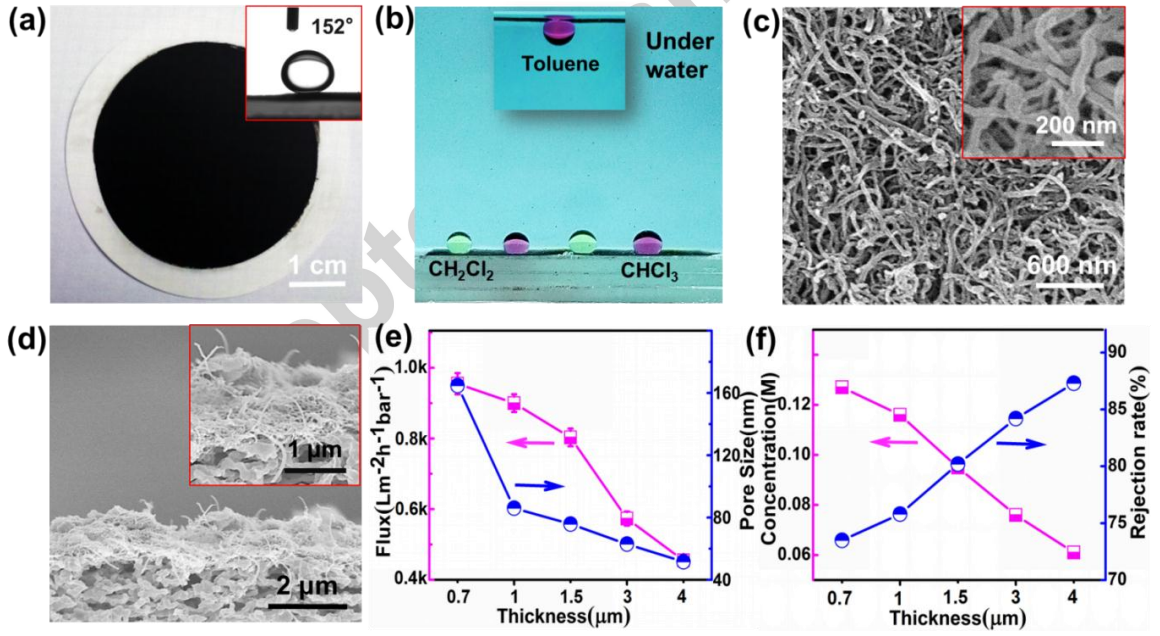

Fig. 2. (a) PAA-CNTs membrane (The inset is the underwater contact angle for CH_2Cl_2). (b) Underwater superoleophobic wettability of the membrane for CH_2Cl_2, $CHCl_3$ and toluene. SEM images of the surface (c) and cross-section (d) of the membrane. (e) The pore sizes and flux of PAA-CNTs membrane with different thickness. (f) The interception

behaviors of PAA-CNTs membrane with different thickness for 40 nm of Au Nanoparticles.

Pd@Pt nanoparticle with about 40 nm diameter serves as a representative for catalytic decomposition of organic dyes pollutes (Fig. S3) and is loaded into CNT membrane by simple filtration (Fig. 3a). The microstructures of resultant composite membrane were characterized by SEM and energy dispersive X-ray (EDX) spectroscopy. It is clearly seen that a large amount of Pd@Pt nanoparticles distributed densely on the whole network membrane. Partial nanoparticles are embedded closely inside the CNTs membrane as well as depositing on the surface (Fig. 3b, 3c). In addition, the distribution of nanoparticles in the membrane was verified by EDX spectroscopy (Fig. 3d). Pd, Pt elements dispersed uniformly on the whole membrane without remarkable large aggregation, indicating highly dispersive distribution of nanoparticles. The good dispersion of Pd@Pt nanoparticles in the membrane ensures their distinct catalytic ability.

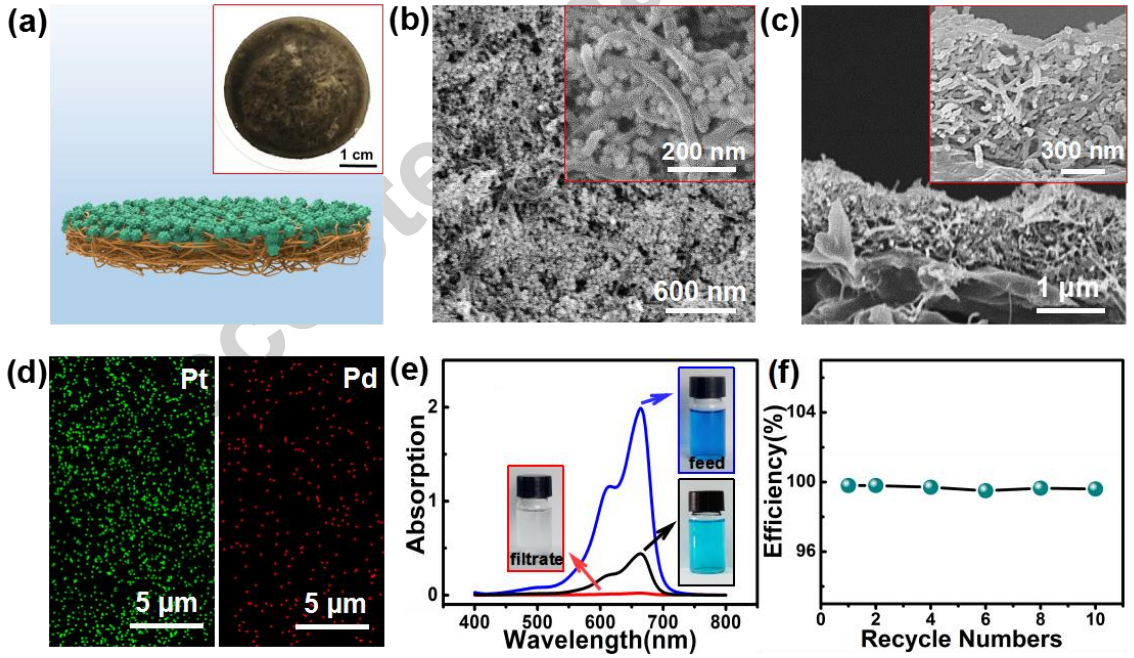

Fig. 3. (a) The schematic structure and photograph of Pd@Pt/PAA-CNTs membrane. (b, c) SEM images of the surface and cross-section of Pd@Pt/PAA-CNTs membrane. (d) Elemental mapping images of Pt (green) and Pd (red) in Pd@Pt/PAA-CNTs membrane. (e) The absorption of MB in feed (blue) and filtrate solution passing through pristine

CNT membrane (black) and Pd@Pt/PAA-CNTs membrane. (f) The general separation efficiency of the membrane in different recycling numbers.

To test the catalytic separation ability of the composite membrane for organic pollutes, methylene blue (MB) aqueous solution degradation tests is selected as a model. 10 mL of mixed feed solution containing MB (12 mg/L) and $NaBH_4$ (0.12 g/L) were poured into the filtration setup and filtrated under vacuum (Fig. S4). The filtrated solution was collected to evaluate the degradation efficiency of the membrane. Upon passing through the composite membrane, blue MB solution transfer rapidly into colorless solution [38] (the inset in Fig. 3e). In the absorption spectra, filtrated solution almost does not show the typical absorption peak of MB, indicating good separation ability of Pd@Pt/PAA-CNTs membrane for MB. The separation efficiency of the composite membrane for MB is quantitatively confirmed by virtue of the standard curves between typical absorption at 664 nm and solution concentration (Fig. S5). The general separation efficiency is defined as $100 \times (C_0 - C) / C_0$ [39, 40], where the C_0 and C represent the MB concentration of initial and after Pd@Pt/PAA-CNTs membrane filtration, respectively. The general separation efficiency of Pd@Pt/PAA-CNTs membrane is approximately 99.8% for 12 mg/L MB solution (Fig. 3f), indicating rapid in-flow catalytic performance during separation. After ten times of separation cycle, the degradation efficiency remained almost unchanged.

It is also well-known that CNT has inherent absorption capacity for some organic dyes. To accurately evaluate the catalytic effects of Pd/@Pt, pristine CNT membrane was used as a referenced membrane to investigate the absorption ability of CNT for MB during separation. After the MB aqueous solution passing through a pristine CNTs membrane, the filtrated solution was collected to evaluate the absorption efficiency based on the standard curves of absorption and concentration (Fig. S5). It is found that the adsorption efficiency of pristine CNT membrane for MB is about 79.1% (black line in Fig. 3 e). The inset picture of filtrate solution in Fig. 3 e shows the blue color, implying

remaining MB after passing through pristine CNT membrane. Therefore, the catalytic degradation efficiency of the composite membrane is about 20.7%. The synergistic effects of Pd@Pt nanoparticles and PAA-CNTs membrane lead to the considerable separation efficiency for MB. This multi-functional membrane also exhibits rapid and stable catalytic performance during separation (Fig. 3 f). After ten times of separation cycle, the degradation efficiency remained almost unchanged.

This multi-layered assembled structure and loading mode via steric hindrance or interception effects allows load various catalytic nanoparticles without specific surface modification. For example, PAA-CNTs composite membranes attached with Au nanoparticles (averaged size 40 nm) are also suitable to effectively decompose toxic 4-NP organic. Au nanoparticles serve as a catalyst for transforming 4-NP into 4-aminophenol in the presence of reductive $NaBH_4$. When the feed aqueous solution containing 2.5 mM of 4-NP and 0.25 M of $NaBH_4$ passes through PAA-CNTs/Au membrane under a low flux (104 L $m^{-2}h^{-1}bar^{-1}$), there is very low content of 4-NP remaining in the filtrate solution (Fig. S6). The purification behaviors of these composite membranes indicate loading catalytic nanoparticles based on interception can effectively decompose organic pollutes during dynamic separation. The convenient loading manners combined with efficient catalytic features endow the composite membranes with flexible applicability for practical wastewater purification.

In addition, the stability of nanoparticles in the composite membrane during the separation process is studied. The catalytic behaviors of the composite is used to evaluate the stability of nanoparticles after repeated using. During ten times cycles of separation, absorption intensity of filtrate solution do not show remarkable changes (Fig. S7 a), which indicates the catalytic performance of the membrane exhibit hardly changes. In addition, the elemental mapping images of Pt in the membrane is similar with the original state after ten cycles of separation. The number of nanoparticles do not decrease significantly (Fig. S7 b and c). It is considered that the nanoparticles can be stably trapped in the membrane. After intercepting 40 nm of nanoparticles (15 mL solution containing about 1.6×10^{-9} mol nanoparticles), the pore sizes of 1-μm-thick CNTs membrane decrease distinctly from 81.3 nm to 46.2 nm (Fig. S8). Besides, the

nanoparticles overlapped with each other and form large-sized assembly anchored on CNT (Fig. 3b). It is not easy for these nanoparticles or the assembly to move in the winding holes of the composite membrane. These results indicate the loaded nanoparticles in the membrane have high resistance against water flushing and are stable enough to be used repeatedly.

3.3. Oil/water emulsion separation and catalytic decomposition

To avoid the fouling on catalytic nanoparticle during separation, a layer of PAA-CNTs network membrane deposits uniformly on Pd@Pt/PAA-CNTs membrane (Fig. 4a). In the SEM images, the achieved composite membrane still has porous network structures and many catalytic nanoparticles are embedded densely into the membrane, forming a multilayer composite membrane with nanoparticles interlayer (Fig. 4b and 4c). The superhydrophilic/underwater superoleophobic surface consisting of PAA-CNTs makes the PAA-CNTs/Pd@Pt/PAA-CNTs membrane suitable for oil/water emulsion separations. Tween-80 stabilized toluene-in-water emulsion is taken as an example to evaluate the emulsion separation ability of the composite membrane. The emulsion separation is performed under 0.09 MPa of vacuum pressure. For oil-in-water emulsions, the PAA-CNTs/Pd@Pt/PAA-CNTs membrane only allows water phase to pass freely due to its underwater superoleophobic surface (Fig. 4d). It is found that heterogeneous feed emulsion transformed into colorless clear solution after filtration (Fig. 4e and 4f, inset). To examine the separation performance, the filtrated solution was further examined by optical microscopy. It is observed that many oil droplets disappear upon separation and there are almost not any large-sized droplets in the collected filtrate solution (Fig. 4e and 4f). The diameter analysis results indicate that only small sized of oil droplets below 14 nm remain in the filtrated solution, showing outstanding oil/water emulsion separation performances.

The reliability of the PAA-CNTs/Pd@Pt/PAA-CNTs hybrid membrane was verified by repeated treatment of toluene-in-water emulsion. After every cycle, the PAA-CNTs/Pd@Pt/PAA-CNTs membrane was refreshed with a small quantity of ethanol.

As shown in Fig. 4g, the flux of the composite membrane almost stays the same even after 10 cycles, which indicates excellent recycled separation performance of the PAA-CNTs/Pd@Pt/PAA-CNTs membrane. During ten cycles of separation, the oil contact angles (OCAs) of the membrane in water decrease slightly from 152° to 150°, showing stable surface wettability and reproducible oil/water separation behavior.

In order to investigate the separation ability of the membrane for real oil, soya-bean oil is selected as an example of plant oil (**Fig. S9**). After passing through the PAA-CNTs Pd@Pt/PAA-CNTs membrane, it is clearly shown that heterogeneous soya-bean oil-in-water feed emulsion transformed into colorless clear solution (**Fig. S9 a and b**). The micron-sized oil droplets in the feed are removed completely and there is only tiny droplets below 10 nm remained in the filtrated solution (**Fig. S9 c**). These results indicate the excellent separating ability of the composite membrane for plant oil-in-water emulsions. Besides, the underwater contact angles of composite membrane change slightly during ten times of recycling separation (**Fig. S9 d**), indicating stable surface wettability and good reproducibility for plant oil/water separation. Therefore, these CNT composite membranes can treat normally plant oil contained emulsions as well as organic solvents.

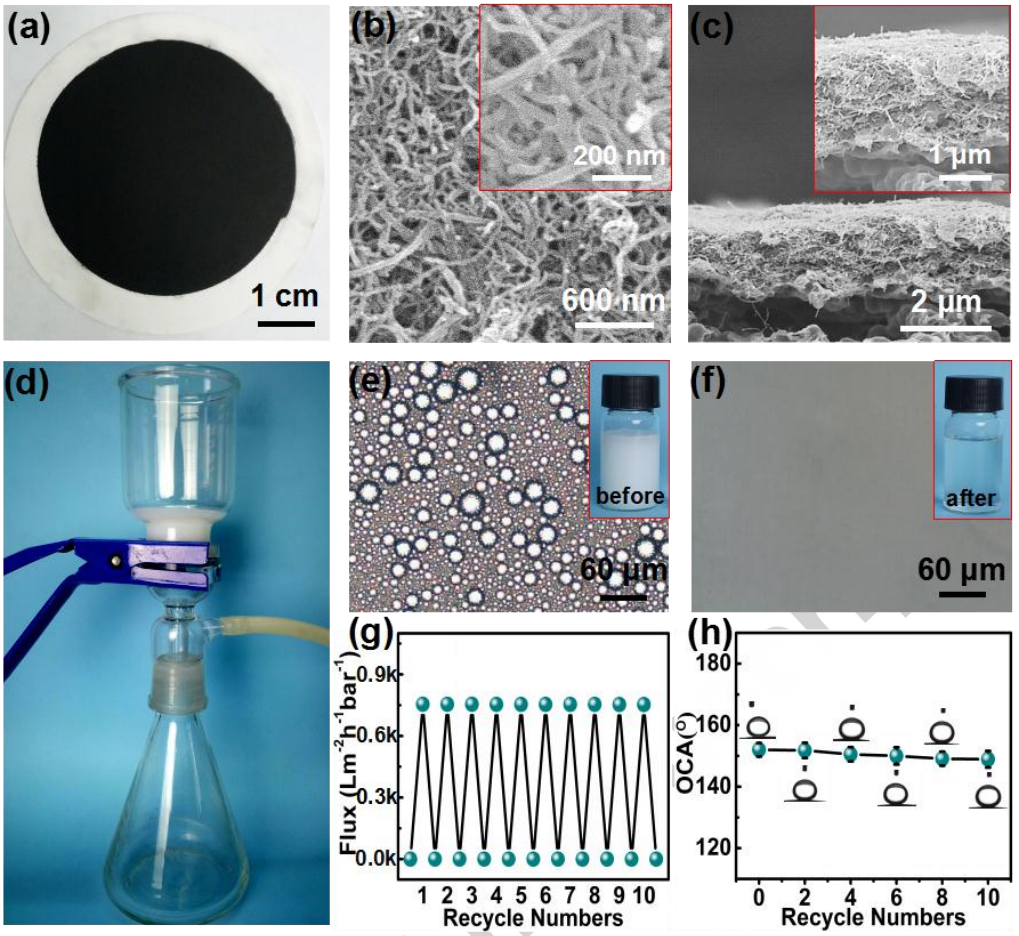

Fig. 4. (a) Photograph of the PAA-CNTs/Pd@Pt/PAA-CNTs composite membrane. (b, c) SEM images of the surface and cross-section of the composite membrane. (d) Toluene-in-water emulsion separation setup. Optical image of feed emulsion (e) and filtrated solution (f). The fluxes (g) and water contact angles (h) of the membrane during ten times recycles.

Owe to the demulsification during oil/water separation, surfactant is easy to adsorb on the membrane surface and change the membrane wetting property, which will remarkably affect the separation performance. The separation flux and efficiency variation of the composite membrane in demulsification process is investigated to evaluate the separation ability. When the composite membrane (about 15.0 cm^2 area) suffers from continuous separation of toluene-in-water emulsion without washing, the separation efficiency reduces clearly due to the absorbed surfactant in demulsification process. It is found the separation efficiency decrease from 99.3% to 91.3% and 85.4% in first three-time

separation (Fig. 5 a), and then reduces to a minimum value of 83.3% after five times separation. Simultaneously, the flux decrease distinctly from 760 to 430 $L \cdot m^{-2}\ h^{-1}\ bar^{-1}$ (Fig. 5 b).

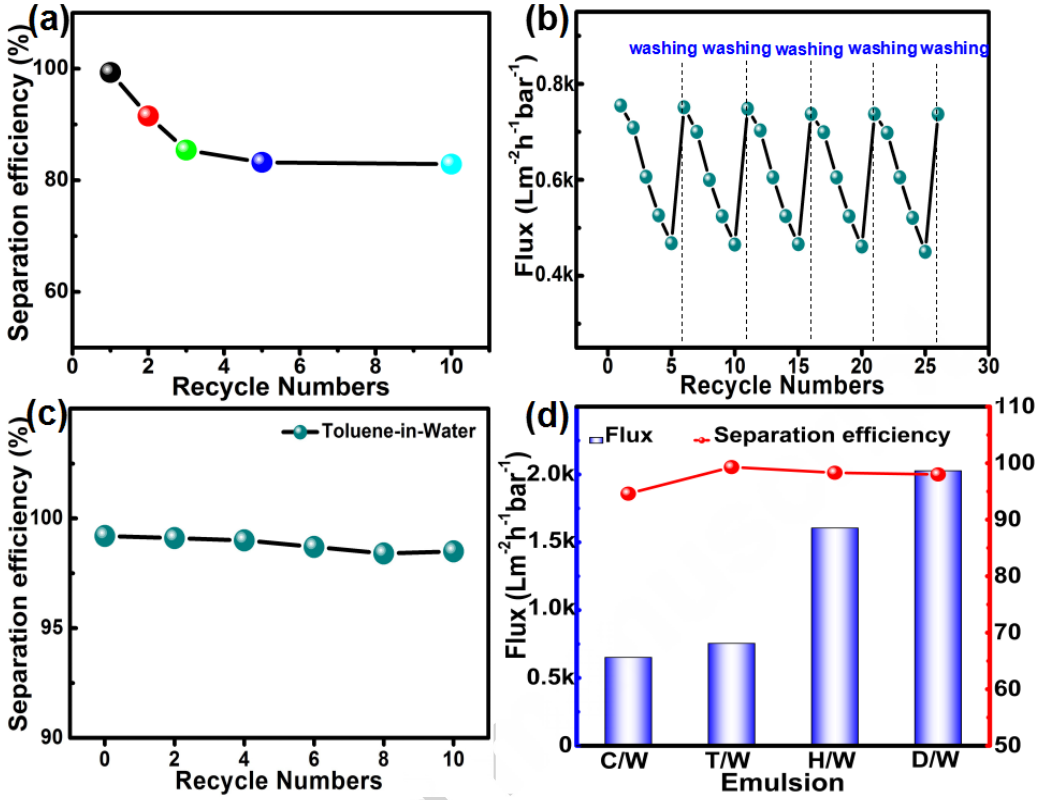

Fig. 5 The separation efficiency (a) and fluxes (b) variation of the PAA-CNTs/Pd@Pt/PAA-CNTs membrane in different continuous separation recycles without washing. (c) The recycled separation efficiency of the composite membrane after washing in each cycles. (d) The separation performance of the composite membrane for other organic solvent emulsion.

In the first five times recycle of treating 50 mL emulsion (containing 1.68 mL of oil and 0.5 g of Tween 80), the separation efficiency of the membrane decrease clearly by 11.1%. The released oil and surfactant in successive demulsification process did not lead to a distinct reduction in separation efficiency although the flux decreases further. Therefore, the maximum separation capacity of the membrane allow treating normally 100 mL emulsion (containing 3.3 % v/v oil phase) with separation efficiency above 83%. After washing by ethanol in each cycle, the flux and separation efficiency reserve almost

to the original state and show slight change even after 25 times of cycles (Fig 5a, c). The PAA-CNTs/Pd@Pt/PAA-CNTs membrane showed stable separation flux. The composite membrane also can treat effectively other emulsions including chloroform-in-water, hexane-in-water and dichloromethane-in-water (Fig. 5d, Fig. S10). When all the three emulsions pass through the membrane, there are only small sized oil droplets around 10 nm in the filtrate solution. The separation efficiency of the composite membrane for these emulsions is much higher than 95 %. Meanwhile, the separation efficiency for toluene-in-H_2O emulsion reach as high as 99.2 %. But the separation fluxes for these four emulsion are different distinctly. The fluxes for separating $CHCl_3$-in-H_2O and tolune-in-H_2O emulsion is lower than 750 L m^{-2} h^{-1} bar^{-1} while the separating flux for CH_2Cl_2-in-H_2O emulsion is as high as 2000 L m^{-2} h^{-1} bar^{-1}.

In order to further investigate the catalytic decomposition performance of PAA-CNTs/Pd@Pt/PAA-CNTs membrane during oil/water separation, the toluene-in-water emulsion containing MB is used as a model of polluted oily wastewater. After passing through the composite membrane, the organic droplets in feed emulsion are removed completely (Fig. 6a and 6b) and there are only small sizes of colloids below 11 nm in the filtrated solution (Fig. 6c). Moreover, blue heterogeneous emulsion simultaneously changes into colorless transparent solution. In the UV/vis absorption of filtrated solution, there is nearly no remarkable featured peaks of MB (Fig. 6d), indicating the MB molecules are almost removed completely during oil/water separation. According to the standard curves (Fig. S5b), the concentration of MB in filtrate solution can be calculated precisely and determine the general separation efficiency of the composite membrane. When the emulsion containing MB with concentration below 30 mg/L pass through the membrane, the general separation efficiency approaches to 99.3% for MB, attributing to the absorption and effective catalytic effects of Pd@Pt nanoparticles (Fig. 6d). When the content of MB in emulsion exceeds 30 mg/L, the separation efficiency decreases gradually and reaches about 93% for treating 60 mg/L MB (Fig. 6e). In a whole, it is expected that PAA-CNTs/Pd@Pt/PAA-CNTs composite membrane can also be recycled for removing MB based on the absorption of CNT and catalytic degradation performance of Pd@Pt. Moreover, the underwater contact angles of

PAA-CNTs/Pd@Pt/PAA-CNTs composite membrane for organic solvents show no remarkable changes after ten times of recycling oil/water separation. The stable surface wettability and catalytic ability allows PAA-CNTs/Pd@Pt/PAA-CNTs composite membrane be used repeatedly in treating polluted oily wastewater.

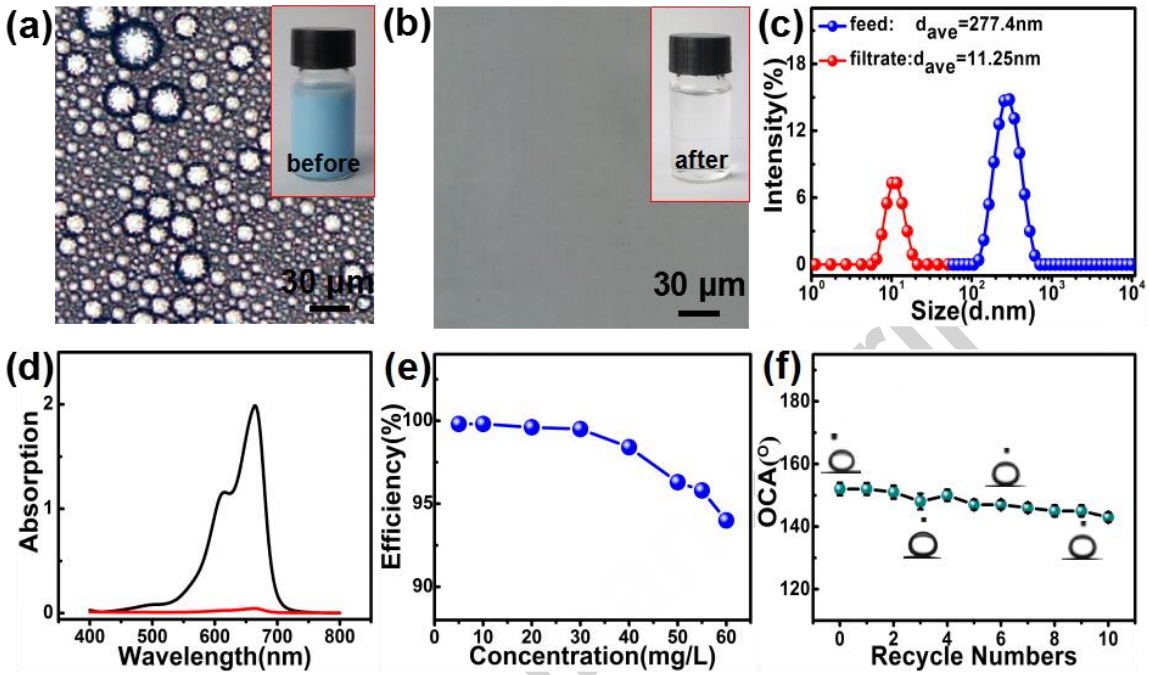

Fig. 6. Oil/water emulsion separation and catalytic performance of PAA-CNTs/Pd@Pt/ PAA-CNTs membrane for toluene/water emulsion containing MB. The optical images of (a) feed emulsion and corresponding filtrated solution (b). Dynamic light scattering diameter analysis (c) and UV/vis absorption (d) of the emulsion and corresponding filtrated solution. (e) General separation efficiency of the membrane for different contents of MB. (f) Underwater oil contact angles in the ten times of separation recycles.

4. Conclusions

In summary, a robust multifunction CNT composite membrane has been fabricated by simple filtration method based on interception effects of CNTs network film. The CNTs network membranes show controllable nanoscale porosity dependent on its thickness, which allows CNTs membrane load stably with catalytic nanoparticles via

simple filtration. It is simplify the construction process and make it very convenient to alter the needed catalytic nanoparticles according to practical pollutants. The prepared superhydrophilic/ underwater superoleophobic composite membrane not only effectively separate various oil-in-water emulsion and catalytically decompose the organic pollutes in water during dynamic separation process. The separation efficiency approach to 99% while the dynamic catalytic degradation for model methylene blue reach about 99.8%. Moreover, the composite membrane also shows outstanding durability and catalytic recyclability. The convenient fabrication and effective oily wastewater purification performance make the PAA-CNTs/Pd@Pt/PAA-CNTs composite membranes have a greatly promising potential in practical applications of agricultural and industrial wastewater treatments.

Acknowledgements

The research was supported by International Science and Technology Cooperation and Exchange Program in Shaanxi Province (2016KW-052), Special Fund for Basic Scientific Research of Central Colleges, Chang'an University (300102318403), Natural Science Foundation of China (51603219, 51603216, 51573203), Bureau of Frontier Science and Education of Chinese Academy of Sciences (QYZDB-SSWSLH036), Youth Innovation Promotion Association of Chinese Academy of Sciences (2016268, 2017337), State Key Laboratory for Modification of Chemical Fibers and Polymer Materials Donghua University (LK1615) for financial support.

Author Contributions

Appendix A. Supplementary data

Supplementary data associated with this article can be found in the online version at http://dx.doi.org/XXX.

References

[1] K. Fent, A.A. Weston, D. Caminada, Ecotoxicology of human pharmaceuticals, Aquat. Toxicol. 76 (2006) 122-159.

[2] Z. Aksu, Application of biosorption for the removal of organic pollutants: a review, Process Biochem. 40 (2005) 997-1026.

[3] M.A. Shannon, P.W. Bohn, M. Elimelech, J.G. Georgiadis, B.J. Marinas and A.M. Mayes, Science and technology for water purification in the coming decades, Nature 452 (2008) 301-310.

[4] Z. Chu, Y. Feng and S. Seeger, Oil/water separation with selective superantiwetting/ superwetting surface materials, Angew. Chem. Int. Ed. 54 (2015) 2328-2338.

[5] Ya. Cai, D. Chen, N. Li, Q. Xu, H. Li, J. He and J. Lu, A facile method to fabricate a double-layer stainless steel mesh for effective separation of water-in-oil emulsions with high flux, J. Mater. Chem. A 4 (2016) 18815-18821.

[6] Ya. Cai, D. Chen, N. Li, Q. Xu, H. Li, J.i He and J. Lu, Nanofibrous metal-organic framework composite membrane for selective efficient oil/water emulsion separation, J. Membr. Sci. 543 (2017) 10-17.

[7] S. Nagappan and C.-S. Ha, Emerging trends in superhydrophobic surface based magnetic materials: fabrications and their potential applications, J. Mater. Chem. A 3 (2015) 3224-3251.

[8] J. Li, L. Yan, H. Li, W. Li, F. Zha and Z. Lei, Underwater superoleophobic palygorskite coated meshes for efficient oil/water separation, J. Mater. Chem. A 3 (2015) 14696-14702.

[9] J. Li, D. Li, Y. Yang, J. Li, F. Zha and Z. Lei, A prewetting induced underwater superoleophobic or underoil (super) hydrophobic waste potato residue-coated mesh

for selective efficient oil/water separation, Green Chem. 18 (2016) 541-549.

[10] Z. Xue, Y. Cao, N. Liu, L. Feng and L. Jiang, Special wettable materials for oil/water separation, J. Mater. Chem. A 2 (2014) 2445-2460.

[11] S.J. Gao, H. Qin, P. Liu, J. Jin, SWCNT-intercalated GO ultrathin films for ultrafast separation of molecules, J. Mater. Chem. A 3 (2015) 6649-6654.

[12] S. Zhang, F. Lu, L. Tao, N. Liu, C. Gao, L. Feng and Y. Wei, Bio-inspired anti-oil-fouling chitosan-coated mesh for oil/water separation suitable for broad pH range and hyper-saline environments, ACS Appl. Mater. Interfaces 5 (2013) 11971-11976.

[13] W. Lv, Q. Mei, J. Xiao, M. Du, Q. Zheng, 3D multiscale superhydrophilic sponges with delicately designed pore size for ultrafast oil/water separation, Adv. Funct. Mater. 27 (2017) 1704293.

[14] F. Zhang, S. Gao, Y. Zhu, J. Jin, Alkaline-induced superhydrophilic/underwater superoleophobic polyacrylonitrile membranes with ultralow oil-adhesion for high-efficient oil/water separation, J. Membrane Sci. 513 (2016) 67-73.

[15] Z. Xue, S. Wang, L. Lin, L. Chen, M. Liu, L. Feng and L. Jiang, A Novel superhydrophilic and underwater superoleophobic hydrogel-coated mesh for oil/water separation, Adv. Mater. 23 (2011) 4270-4273.

[16] S. Gao, Y. Zhu, F. Zhang, J. Jin, Superwetting polymer-decorated SWCNT composite ultrathin films for ultrafast separation of oil-in-water nanoemulsions, J. Mater. Chem. A 3 (2015) 2895-2902.

[17] I. Ali, New generation adsorbents for water treatment, Chem. Rev. 112 (2012) 5073-5091.

[18] Y. Zhong, T. Li, H. Lin, L. Zhang, Z. Xiong, Q. Fang, G. Zhang, F. Liu, Meso-/macro-porous microspheres confining Au nanoparticles based on PDLA/PLLA stereo-complex membrane for continuous flowing catalysis and separation, Chem. Eng. J. 344 (2018) 299-310.

[19] J. Wang, Z. Wu, T. Li, J. Ye, L. Shen, Z. She, F. Liu, Catalytic PVDF membrane for

continuous reduction and separation of p-nitrophenol and methylene blue in emulsified oil solution, Chem. Eng. J. 334 (2018) 579-586.

[20] C. Gao, Z. Sun, K. Li, Y. Chen, Y. Cao, S. Zhang and L. Feng, Integrated oil separation and water purification by a double-layer TiO_2-based mesh, Energy Environ. Sci. 6 (2013) 1147-1151.

[21] L. Zhang, J. Gu, L. Song, L. Chen, Y. Huang, J. Zhang and T. Chen, Underwater superoleophobic carbon nanotubes/core-shell polystyrene@Au nanoparticles composite membrane for flow-through catalytic decomposition and oil/water separation, J. Mater. Chem. A 4 (2016) 10810-10815.

[22] J. Shi, L. Zhang, P. Xiao, Y. Huang, P. Chen, X. Wang, J. Gu, J. Zhang, and T. Chen, Biodegradable PLA nonwoven fabric with controllable wettability for efficient water purification and photocatalysis degradation, ACS Sustainable Chem. Eng. 6 (2018) 2445-2452.

[23] M.A. Ferguson and J.G. Hering, TiO_2-Photocatalyzed As (III) oxidation in a fixed-bed, flow-through reactor, Environ. Sci. Technol. 40 (2006) 4261-4267.

[24] J. Gu, P. Xiao, J. Chen, J. Zhang, Y. Huang and T. Chen, Janus polymer/carbon nanotube hybrid membranes for oil/water separation, ACS Appl. Mater. Interfaces 6 (2014) 16204-16209.

[25] J. Gu, P. Xiao, J. Chen, F. Liu, Y. Huang, G. Li, J. Zhang and T. Chen, Robust preparation of superhydrophobic polymer/carbon nanotube hybrid membranes for highly effective removal of oils and separation of water-in-oil emulsions, J. Mater. Chem. A 2 (2014) 15268-15272.

[26] J. Gu, P. Xiao, Y. Huang, J. Zhang and T. Chen, Controlled functionalization of carbon nanotubes as superhydrophobic material for adjustable oil/water separation, J. Mater. Chem. A 3 (2015) 4124-4128.

[27] J. Gu, P. Xiao, L. Zhang, W. Lu, G. Zhang, Y. Huang, J. Zhang and T. Chen, Construction of superhydrophilic and under-water superoleophobic carbon-based membranes for water purification, RSC Adv. 6 (2016) 73399-73403.

[28] X. Lu, A. Dandapat, Y. Huang, L. Zhang, Y. Rong, L. Dai, Y. Sasson, J. Zhang and T. Chen, Tris base assisted synthesis of monodispersed citrate-capped gold nanospheres with tunable size, RSC Adv. 6 (2016) 60916-60921.

[29] Y. Huang, D. H. Kim, Synthesis and self-assembly of highly monodispersed quasispherical gold nanoparticles, Langmuir 27 (2011) 13861-13867.

[30] G. Guo, D. Yang, C. Wang, S. Yang, "Fishing" polymer brushes on single-walled carbon nanotubes by in-situ free radical polymerization in a poor solvent, Macromolecules 39 (2006) 9035-9040.

[31] S.H. Shim, K.T. Kim, J.U. Lee, W.H. Jo, Facile method to functionalize graphene oxide and its application to poly(ethylene terephthalate)/graphene composite, ACS Appl. Mater. Interfaces 4 (2012) 4184-4191.

[32] Y. Lei, G. Gao, W. Liu, T. Liu, Y. Yin, Synthesis of silver nanoparticles on surface-functionalized multi-walled carbon nanotubes by ultraviolet initiated photo-reduction method, Applied Surface Science 317 (2014) 49-55.

[33] D. Yang, J. Hu, C. Wang, Synthesis and characterization of pH-responsive single-walled carbon nanotubes with a large number of carboxy groups, Carbon 44 (2006) 3161-3167.

[34] J. Li, S. Tang, L. Lu, H.C. Zeng, Preparation of nanocomposites of metals, metal oxides, and carbon nanotubes via self-assembly, J. Am. Chem. Soc. 129 (2007) 9401-9409.

[35] D. Yan, F. Wang, Y. Zhao, J. Liu, J. Wang, L. Zhang, K.C. Park, M. Endo, Production of a high dispersion of silver nanoparticles on surface-functionalized multi-walled carbon nanotubes using an electrostatic technique, Mater. Lett. 63 (2009) 171-173.

[36] S. Kundu, Y. Wang, W. Xia, M. Muhler, Thermal stability and reducibility of oxygen-containing functional groups on multiwalled carbon nanotube surfaces: a quantitative high-resolution XPS and TPD/TPR study, J. Phys. Chem. C 112 (2008) 16869-16878.

[37] Y. V. Butenko, S. Krishnamurthy, A.K. Chakraborty, V.L. Kuznetsov, V.R. Dhanak, M.R.C. Hunt, L. Siller, Photoemission study of onionlike carbons produced by annealing nanodiamonds, Phys. Rev. B 71 (2005) 075420.

[38] G. Fu, L. Tao, M. Zhang, Y. Chen, Y. Tang, J. Lin, T. Lu, One-pot, water-based and high-yield synthesis of tetrahedral palladium nanocrystal decorated graphene, Nanoscale 5 (2013) 8007-8014.

[39] Y. Yang, G. Hu, F. Chen, J. Liu, W. Liu, H. Zhang, B. Wang, An atom-scale interfacial coordination strategy to prepare hierarchically porous Fe_3O_4-graphene frameworks and their application in charge and size selective dye removal, Chem. Commun. 51 (2015) 14405-14408.

[40] F. Chen, A.S. Gong, M. Zhu, G. Chen, S.D. Lacey, F. Jiang, Y. Li, Y. Wang, J. Dai, Y. Yao, J. Song, B. Liu, K. Fu, S. Das, L. Hu, Mesoporous, Mesoporous, three-dimensional wood membrane decorated with nanoparticles for highly efficient water treatment, ACS Nano 11 (2017) 4275-4282.

Highlight

- Multifunctional superhydrophilic/underwater superoleophobic CNTs composite membrane
- Effectively and simply loaded catalytic nanoparticles via interception effect
- The dependences of interception on the membrane porosity and thickness are studied
- Decompose organic pollutes during oil/water emulsion separation
- High emulsion separation efficiency and catalytic decomposition efficiency.